

Study of Cross-Contamination in Multi-Chamber PVD Systems Used for High-Throughput Seed Layer Deposition

Modern WLP applications require PVD systems that can deliver low and stable contact resistance (R_c) at high throughput. HEXAGON is an excellent candidate to fulfill this role. This study demonstrates that chamber-to-chamber cross-talk during continuous run is negligible compared to the residual outgassing of the etched wafer itself as explained by **Kay Viehweger** from Fraunhofer IZM-ASSID, Germany, and Evatec's Senior Process Engineer, **Dr. Patrick Carazzetti**.

Abstract

Higher interconnect density in WLP applications increases the importance of interconnect quality, measured by contact resistance (R_c). UBM and RDL metallization are key steps. HEXAGON shows 50% lower R_c and 40% higher throughput than the CLUSTERLINE®. Cross-contamination mainly comes from residual outgassing of etched PBO wafers.

Introduction

Wafer-level packaging (WLP) technologies play a key role in supporting the continuous miniaturization, increased functionality and better power efficiency required by the ever more sophisticated system-on-chip (SoC) and system-in-package (SiP) architectures [1,2]. The downscaling of the critical design dimension and the concomitant increase of I/O density per unit area, has increased the need for a tighter control of the contact resistance (R_c). R_c is referred as the ohmic resistance between the uppermost level of the active circuitry and the metal routing to the bumps. In fact, R_c is directly related to the performance of the packaged device, such as the overall power consumption and signal integrity [3-5]. High-volume manufacturing (HVM) relies on magnetron sputtering for the deposition of adhesion/seed layers that are necessary for the subsequent formation of under bump metallization (UBM) and redistribution layers (RDL). The sputtered PVD stack primarily provides the adhesion function to the underlying pad and organic dielectric passivation, and also a conductive layer for electroplating. Prior to the sputter deposition, state-of-the-art multi-chamber PVD systems perform dedicated pre-treatment steps to improve the metal adhesion to the dielectric. First, the degas step drives out moisture from the dielectric film, which is especially necessary for hydrophilic organic materials, such as Polyimide (PI) or Polybenzoxazole (PBO) [6-8]. This is to avoid that excessive water molecules re-emerge during the subsequent fabrication steps. Secondly, the wafer is sputter cleaned using a mild Argon plasma bombardment to remove oxides from the metal contacts (usually Al or Cu pads) formed through the organic passivation. This etch clean, is typically an inductively-coupled plasma (ICP) process operating at low bias voltage (<600 volts) to avoid device damage. Next, without breaking vacuum, the wafer undergoes the sequential deposition of the Ti-adhesion and Cu-seed layers. The load of organic volatile byproducts generated during the non-selective

Ar sputter etching must be efficiently removed from the system to avoid contamination of the other process stations. Since the final device performance is measured only upon completion of the entire WLP process, it is critically important to manage the contamination level and to ensure that especially the Ti-adhesion layer capping the I/O contacts, is deposited in a clean environment that prevents oxide re-growth and contamination from hydrocarbon species.

Previous research presented a benchmark of throughput and R_c performance of two competing PVD systems architectures used in the manufacturing of UBM and RDL metallization. These PVD systems are the HEXAGON and the CLUSTERLINE®, respectively. Data generated in wafer-level chip-scale packaging (WLCSP) have demonstrated that the HEXAGON can consistently deliver 50% lower R_c baseline for a corresponding 40% higher throughput [9]. Further hardware developments of the HEXAGON platform were done to boost its handling speed. This improvement has demonstrated that the HEXAGON can maintain low and constant R_c values even at record throughput of 80.0 wafers/hour [10]. Beside the overall better performance obtained on the HEXAGON compared to the CLUSTERLINE®, there is an aspect of the former platform that has not been sufficiently investigated. In fact, the indexing concept itself, based on the simultaneous transfer of all wafers, would make this platform critically exposed to cross-talk between the different process stations. This can result in an excessive contamination of the PVD chambers, primarily due to the load of organic volatiles species propagating from the ICP sputter etch chambers. The consequence could be the contamination of the metal interfaces, which may adversely impact the R_c of the fabricated device.

This work presents a side-by-side comparison of the cross-contamination dynamics occurring in the HEXAGON and CLUSTERLINE® PVD systems employed in their current HVM

configuration. Residual Gas Analysis (RGA) is used to characterize the level of contamination in two strategically important locations of both platforms. These are the vacuum transport module (VTM) and the Ti deposition chamber.

Hardware Characteristics and Process Strategies

The main hardware characteristics, process strategies and performance of the two platforms are compared in Table I. More than a decade ago, the “arctic” ICP etch chamber was introduced to tackle new process challenges arising from the poorly vacuum compatible organic passivation materials, which were starting to see widespread use as dielectric layers in WLCSP applications [9]. The concept basically consisted in actively cooling the process environment by means of an external chiller unit supplying coolant fluid to the pedestal and the chamber shields.

Essential Hardware Characteristics, Process Strategies and Performance of the PVD Platforms Presented

The chilled pedestal coupled with Argon back-gas provides in-situ cooling to the substrate during process. Whereas the active cooling of the metal shields counterbalances the heating effect induced by the plasma process, thereby mitigating additional outgassing from the organic material residues already present in the chamber. In addition to the active cooling, the pumping efficiency of the chamber was also improved. Furthermore, aluminium pasting was introduced as a periodic conditioning procedure to keep R_c low and stable and to extend the shields lifetime [11]. The Atmospheric Batch Degas (ABD) was developed to deal with heavily outgassing substrates, such as the Epoxy-mold compound (EMC) used in Fan-Out wafer-level packaging (FOWLP) applications [9]. In the ABD, a batch of wafers is loaded into a heated metal cassette and exposed to a laminar flow of N₂ for a minimum time of 20 minutes.

Several advantages inherent to its configuration, as well as the dedicated process strategies allow the HEXAGON platform to reach best-in-class R_c at higher throughput compared to the CLUSTERLINE®. Two aspects which are believed to play a key role are discussed hereafter. First, the faster chamber-to-chamber transfer time allows to minimize the time interval between the end of the ICP sputter etch and the beginning of the sputter deposition of the Ti-adhesion layer. This is believed to decrease the risks of recontamination or reoxidation of the cleaned contacts. Secondly, the strategy of splitting the ICP etch amount in two chambers is beneficial to contain the residual outgassing load in the first chamber, while the contact cleaning is completed in the second chamber relatively free from volatile contaminants.

Typically, a multi-chamber PVD system operates in a regime where the throughput limitation comes from the longest sequence executed in one of the process chambers. Steady-state operation mode is achieved when consecutive batch of wafers are processed in the system without interruptions. The residence time in the ABD does not represent the bottleneck as long as neither its capacity, nor the process time impact the regular flow of wafers to sustain continuous loading of the airlock. The handling speed of the platform comes into play during the chamber-to-chamber wafer transfer. From the R_c standpoint, it is therefore strategically important to setup the process flow in such a way to minimize the transfer time occurring between the end of the ICP sputter etch and the beginning of the Ti deposition. Practically, this is achieved by imposing the etch sequence to become the time bottleneck of the entire flow. In the case of the HEXAGON, where the etch amount is split over two chambers, the process sequence is programmed in such a way that the second chamber becomes the bottleneck.

Topic	Platform type	
	HEXAGON	CLUSTERLINE®
Transport in atmosphere	<ul style="list-style-type: none"> Combined Gantry / SCARA 5-axis robot 	<ul style="list-style-type: none"> Combined Gantry / SCARA 5-axis robot
Transport in vacuum	<ul style="list-style-type: none"> Central servo motor with revolving carousel 	<ul style="list-style-type: none"> Bisymmetric arm robot
Wafer transfer time in vacuum [sec]	<ul style="list-style-type: none"> 13.0 (older generation) 8.0 (new generation) 	<ul style="list-style-type: none"> 28.0 – 30.0
Airlock cycle time [sec]	<ul style="list-style-type: none"> 25.0-28.0 (single unit) Wafer capacity: 1 	<ul style="list-style-type: none"> 50.0-56.0 (2 units operating in parallel) Wafer capacity: 2
Pumping system (high vacuum)	<ul style="list-style-type: none"> Airlock: turbo Process chambers: turbo VTM: turbo and cold traps 	<ul style="list-style-type: none"> Airlock: turbo ICP etch chamber: turbo PVD chambers: Cryo VTM: Cryo
Degas strategy	<ul style="list-style-type: none"> Atmospheric Batch Degas (ABD) for WLCSP & FOWLP 	<ul style="list-style-type: none"> Single-wafer vacuum degas for WLCSP ABD for FOWLP
Cooling station	<ul style="list-style-type: none"> Dedicated process chamber with chilled pedestal, wafer clamp and back-gas 	<ul style="list-style-type: none"> Not implemented
ICP sputter etch strategy (“arctic” chamber)	<ul style="list-style-type: none"> Two serial etch chambers (50/50 split etch amount) Chilled pedestals and metal shields (-30°C) 	<ul style="list-style-type: none"> Single etch chamber Chilled pedestal and metal shields (-30°C)
Aluminium pasting strategy (ICP chamber)	<ul style="list-style-type: none"> Automated by SW, with aluminum plates stored in atmospheric buffer station 	<ul style="list-style-type: none"> Automated by SW, with aluminum plates stored in atm. or vacuum buffer stations
Throughput [wafers/hour]	<ul style="list-style-type: none"> 90-100 (handling limited) 45-55 (process limited^a) 	<ul style="list-style-type: none"> 40-45 (handling limited) 26-34 (process limited^a)
Rc [mΩ] (source OSATs)	<ul style="list-style-type: none"> 7.0 ± 0.3 Al pasting frequency every 10 prod. wafers 	<ul style="list-style-type: none"> 7.5 - 12.0 increased Al pasting frequency

^aDepending on the aluminium pasting frequency.

Thermal model

The typical process-of-records (POR) used in UBM/RDL production are reported in Figure 1 along with the simulated thermal profiles of a 300 mm Silicon wafer. Despite the tool configurations differ by the number of process chambers used, the process output in terms of (1) degas time and temperature, (2) etching amount and (3) PVD stack thickness remains the same. Based on the substrate properties, the thermal model calculates the heating rates of the different plasma processes involved, as well as the cooling rates during transfer and in-situ cooling provided by “arctic” etch and Ar backside gas. In the HEXAGON tool, the first process chamber in vacuum fulfills the role of cooling station. Here the substrate is mechanically clamped to the chilled pedestal for 50 sec. At the same time, Argon is applied at the wafer backside to increase the cooling efficiency. The combination of the cooling step and split etch approach results in a substrate temperature of 145°C (Figure 1a). On the other hand, the absence of the cooling station on the CLUSTERLINE® and the full etch amount performed in a single chamber result in a 40°C higher peak temperature (Figure 1b). In general, a lower temperature after the etching process is another beneficial aspect that helps to reduce outgassing and the related risk of recontamination, thus contributing to a better R_c control. The POR run on the HEXAGON results in a peak temperature of 170°C at a throughput of 54.5 wafers/hour. The CLUSTERLINE® POR reaches a peak temperature of 186°C and 33.3 wafers/hour throughput.

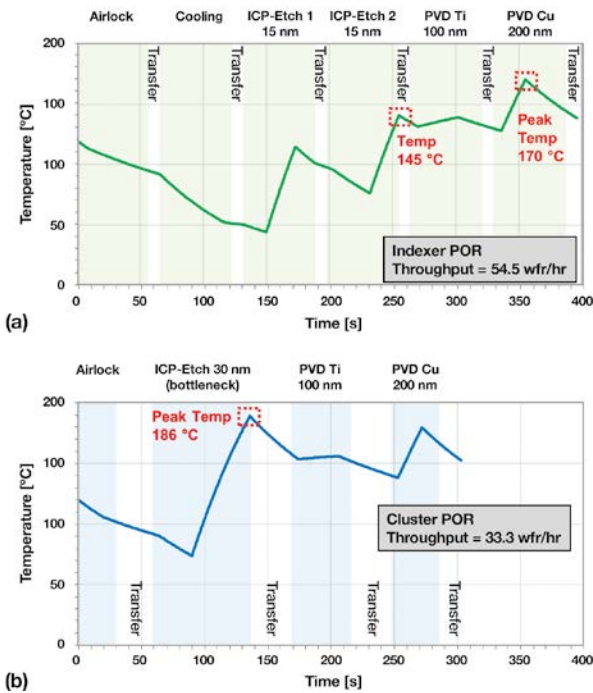


Figure 1a & 1b: Thermal profiles of a 300 mm Silicon wafer processed with UBM/RDL POR on the HEXAGON (a) and on the CLUSTERLINE® (b).

Wafer transfer in the HEXAGON

During process, the chamber pedestal is in the upper position and the cylindrical bellow fixated to the pedestal pushes the wafer carrier against the chamber flange. The isolation of the chamber is realized by compressing the two Viton seals inserted in the upper surfaces of the bellow and in the carrier against the above metal surfaces [12] (Figure 2 (a)). The transfer sequence is

illustrated in Figure 2 (b)-(e). As soon as the bottleneck sequence is completed, the control SW issues the transfer command. The transfer sequence starts by the synchronized pneumatically driven down-stroke movement of all pedestals, which takes approximately 2.0 seconds. This action compresses the chamber bellows and consequently unseals the process environment in regard of the VTM. During the down movement, the wafers are placed on the carriers mounted on the HEXAGON carousel. The carousel plane is situated at an intermediate level between the two extreme positions of the pedestal. When the pedestals are in the lower position, the HEXAGON is free to move. At this moment, the servo motor drives in 3.0 sec the 60°-clockwise rotation of the carousel. As a result, all wafers are transferred simultaneously to the subsequent process station. It is important to note that during the indexing phase, process chambers and VTM share the same vacuum conditions. Next, the synchronized 2.0 sec up-stroke movement of

the pedestals lifts the wafers from the carriers and seals again the chambers from the VTM. Now the wafers are sitting on the chuck top and the process sequence can start. In the new HEXAGON platform with central servo motor, the whole wafer transfer sequence takes approximately 8.0 sec. This is 5.0 sec faster compared to the earlier platform generation with a gear-driven carousel.

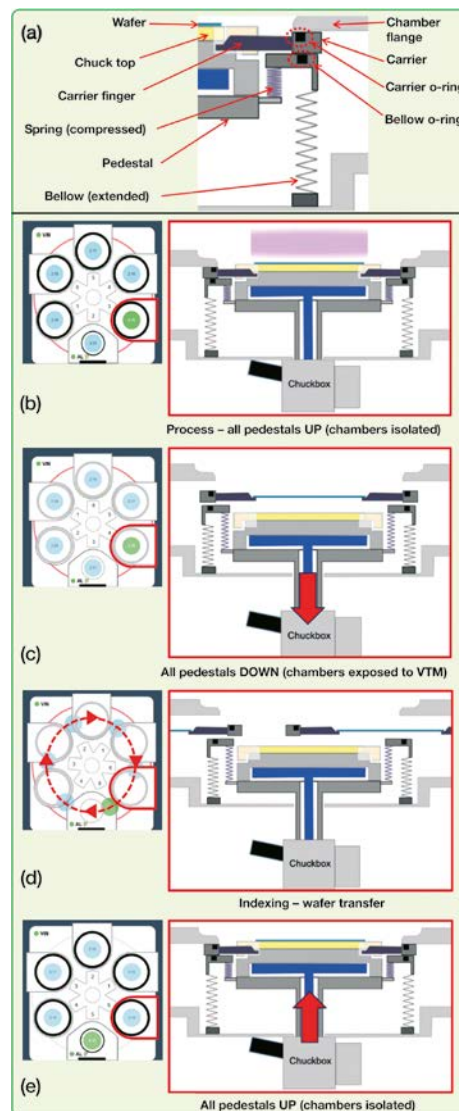


Figure 2: Chamber cross section (a) and wafer transport steps in the HEXAGON with central servo motor (b)-(e).

Wafer transfer in the CLUSTERLINE®

The transfer sequence in the CLUSTERLINE® is illustrated in Figure 3. Up to six process chambers and two airlock units are clustered around the VTM. The latter is equipped with a bisymmetric arm robot performing pick-&-place operation. All process stations and

airlocks are isolated from the VTM by means of individual slit valves. The valve opens prior wafer pick and closes after the next wafer has been placed. Thus, the VTM is exposed to the process chamber environment for a 15.0 sec time interval. The pedestal of the process chamber is actuated by a servo motor, and this is allowed to move only when the slit valve is closed. Both the down and up-stroke movements require approximately 10.0 sec. The total chamber-to-chamber transfer in the CLUSTERLINE® is approximately 30.0-35.0 sec. This corresponds also to the time interval between the end of the ICP sputter etch sequence (flow bottleneck) and the start of the Ti deposition. During steady-state operation, it can be observed that one wafer remains on standby on one of the robot arms until the ICP etch chamber becomes available (Figure 3 (a)). Since the wafer in question was previously degassed in the ABD, its temperature remains in the order of 100°C and thus continues to outgas and contaminate the VTM during its residence.

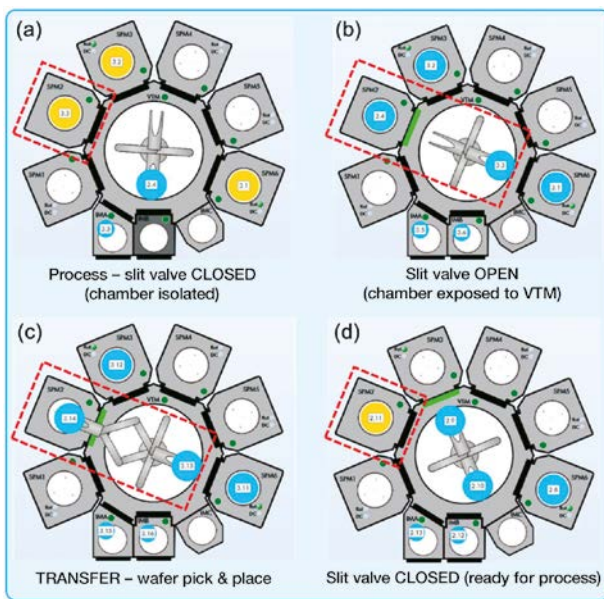


Figure 3: Wafer transport sequence in CLUSTERLINE® with bisymmetric-arm robot in the VTM. Each chamber is isolated from the VTM by means of individual slit valves.

Airlock cycle

Figure 4 compares the airlock performance of both systems. The pressure curves were recorded during a cycle run of SiO₂ wafers. The pumpdown and venting time, as well as the wafer transfer time in vacuum and atmosphere are indicated. The reduced volume and the pumping scheme of the HEXAGON airlock are optimized for fast vent/pump cycle. Typically, the pumpdown time from atmosphere to the vacuum threshold 5.0E-5 Torr requires 10.0 sec. The venting time with N₂ takes approximately 5.0 sec. During the movement of the airlock pedestal followed by the indexing, the pressure measured in the airlock is in the order of 1.0E-5 Torr, meaning two decades higher than the pressure of the VTM (not shown here). This different pressure level in regard of cross-contamination will be discussed in Section IV.

The control SW of the CLUSTERLINE® manages the operation of two airlock units in parallel. Each airlock has a capacity of two substrates. The upper position is reserved for the incoming substrates, which have been previously processed in the ABD. The lower position is reserved for the outgoing wafers, whose

process is complete and are transferred back to the FOUNDRY. The typical pumping time to the vacuum threshold of 5.0E-5 Torr is 25.0 sec and the venting time is 16.0 sec (Figure 4b). The slower pump and vent result in part from the larger airlock volume compared to the HEXAGON design. In the example shown, the base pressure of the airlock approaches 1.0E-5 Torr for a residence time of 40.0 sec. Then, as soon as the slit valve opens to allow the wafer transfer, the airlock pressure drops due to the lower pressure level of the VTM. During the indicated 14.0 sec necessary for placing the outgoing wafer and picking the incoming wafer, the VTM is to some extent exposed to the contamination from the residual atmosphere of the airlock.

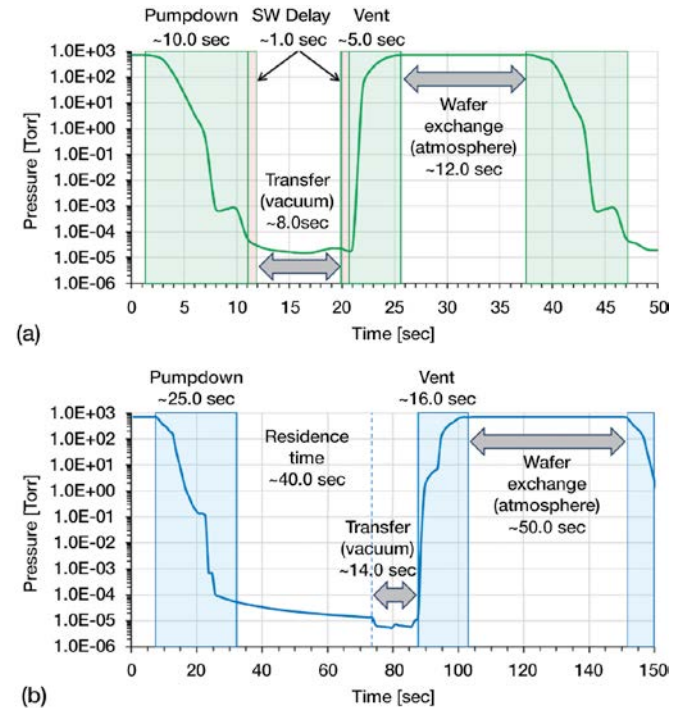


Figure 4a & 4b: Airlock pressure curves indicating pumping/venting and transfer time: HEXAGON (a) and CLUSTERLINE® (b). In both cases SiO₂ wafers were used.

Experimental Method

A series of tests is conducted on 300 mm wafers to characterize the contamination caused by the residual outgassing. RGA measurements are performed with HPQ3 model from MKS, whose upper working limit is 1.0E-3 Torr [13]. RGA devices are installed in two strategically important locations of the PVD platforms, namely the VTM and the Ti deposition chamber. Measurement in the VTM provides information on the outgassing propagating from the process chambers during the time interval when the wafers are in transit. Whereas data collected in the PVD-Ti chamber provides information on the background contamination before the start of the film deposition. Two different sets of wafers were used to execute the test plan summarized in Table II. A batch of 25 Si wafers with 5'000 Å of thermal oxide grown on both frontside and backside was used as a reference of non-outgassing material. A second lot of 25 Si wafers coated with 9.0 µm of PBO was used to mimic the outgassing of real products with organic passivation. RGA data of both wafer lots are presented in Section IV.

Design of Experiment – Datasets Collection

Platform	RGA location	Wafer type (25-wafers run)	
HEXAGON	VTM	SiO ₂	PBO
	PVD-Ti	SiO ₂	PBO
CLUSTERLINE®	VTM	SiO ₂	PBO
	PVD-Ti	SiO ₂	PBO

Figure 5 illustrates the system configuration, the locations of the RGA and the corresponding flow used to process the test wafers. Degas and ICP sputter etch processes were performed according to the POR previously described. In contrast, no metal was sputtered in the PVD chambers, instead the wafers were kept in vacuum for 50.0 sec. The RGA spectra were recorded from 1 to 50 a.m.u. during continuous wafer run.

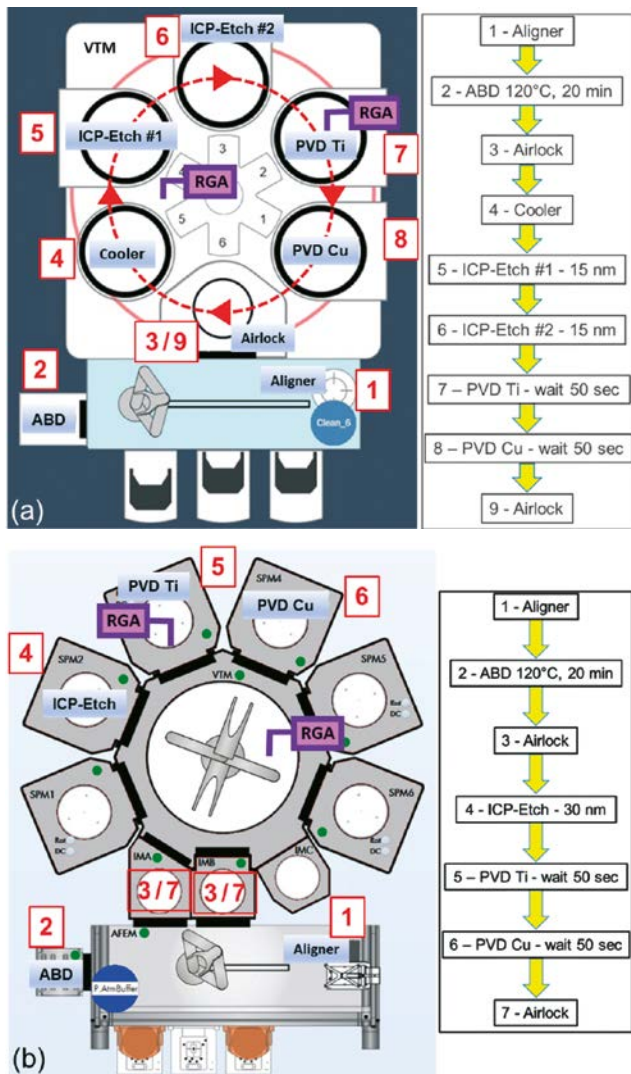


Figure 5: Configuration of the PVD systems used in HVM: HEXAGON (a) and CLUSTERLINE® (b). The process flows executed to run the cross-contamination tests are indicated beside each platform.

Results

Each dataset presented in the next paragraphs refers to a 25-wafers lot. To avoid a too clogged display, each chart is limited to a timespan of 300 sec, which is sufficient to describe accurately the behavior

of the lot. The masses of the different species present in the spectra were identified based on available libraries [14]. The results are presented and discussed based on a selected group of the most prominent masses measured. These are in part originated from the Argon process gas, such as masses 40 and 20, which are attributed to Ar⁺ and Ar⁺⁺. The other masses considered are related to the volatile contaminants. Masses 18, 17 and 16 can be attributed to the presence of water molecules (H₂O⁺) and the corresponding fragments, i.e. HO⁺ and O⁺. However, mass 16 can also be related to the ion CH₄⁺. The presence of organic contaminants is normally indicated by the species with mass 28 (CO⁺) and mass 44 (CO₂⁺). The signal of mass 28 can also be attributed to nitrogen (N₂⁺) as a specie present in the base pressure of the system and in the residual airlock atmosphere. Finally, mass 32, attributed to O₂⁺, is also monitored.

HEXAGON – VTM RGA: SiO₂ vs. PBO Wafers

Figure 6 (a) and (b) displays the RGA spectra measured in the VTM of the HEXAGON during the process of SiO₂ and PBO wafers. The partial pressures of 4 known contaminants are compared in Table III. Masses 16 and 17 are omitted from the table as the former normally shows a marginal partial pressure and the second follows closely the trend of mass 18. Each of the pressure peaks, indicate that a transfer cycle takes place. At the instant t₁ the pedestals move down to allow the rotation of the carousel. This event corresponds to a sharp increase of the VTM pressure. The contributors to this increase are: (1) the residual airlock atmosphere, (2) the residual Ar process gas, and (3) the volatile byproducts generated during the etching process. During transfer, at t > t₁, the VTM pressure is mainly dominated by masses 40 and 20. In the case of PBO wafers, masses 28 and 40 are significantly more prominent than on SiO₂ wafers. This reflects the presence of byproducts generated during etching of this organic film. After transfer, the chambers are again isolated from the VTM environment. The pressure promptly recovers and stabilizes within seconds. At the instant t₂ the Argon species practically disappear from the spectrum and the difference between the wafer types can be seen mainly by the higher partial pressure of masses 28 and 44. In both cases, at t₃ the main contributors to the VTM pressure are masses 18 and 17.

The time interval between consecutive transfer events, e.g., t₁ and t₃, represents the wafer cycle time. When the cycle time is stable and constant, this can be used to calculate the steady-state throughput as indicated below:

$$\text{Throughput} = 3600/\text{cycle time [wafers/hour]} \quad (1)$$

The HEXAGON is running the process outlined in Figure 5a operates at a cycle time of 65.5 sec, which corresponds to a steady-state throughput of 55.0 wafers/hour.

CLUSTERLINE® – VTM RGA: SiO₂ vs. PBO Wafers

Figure 7a and 7b compare the RGA spectra measured in the VTM of the CLUSTERLINE® during the process of SiO₂ and PBO wafers. The partial pressures of the contaminants are reported in Table IV. The steady-state regime is reached when the process stations used by a given process flow are fully populated. This means, for instance, that the transfer history exhibits a periodic behavior throughout the job. In the steady-state conditions reached in this test, the vacuum robot necessitates 52 sec to transfer one-by-one the 5 wafers present in the system at once. The sudden pressure

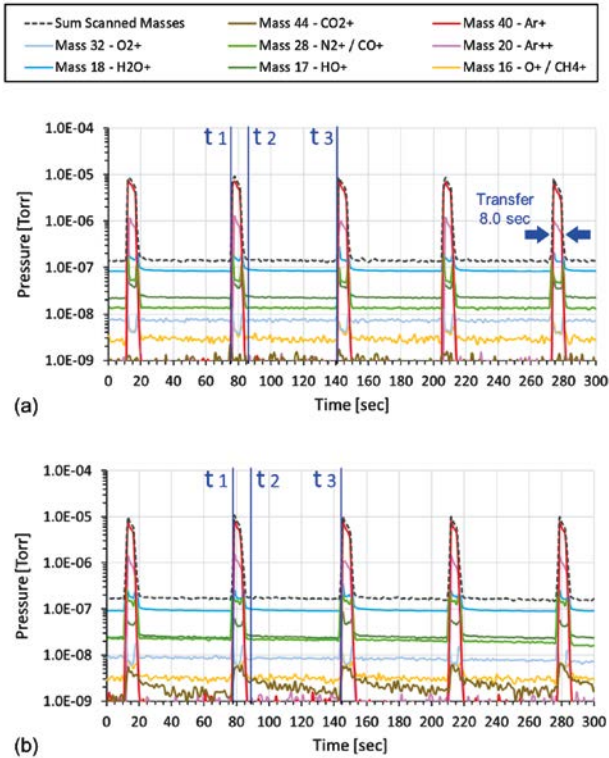


Figure 6: Selected masses measured in the VTM of the HEXAGON system, comparison of SiO₂ wafers (a) vs. PBO wafers (b).

Time flag	Wafer type	Selected masses and partial pressures [Torr]			
		Mass 18	Mass 28	Mass 32	Mass 44
t ₁	SiO ₂	1.71E-7	5.76E-8	4.49E-9	9.56E-10
	PBO	2.5E-7	1.61E-7	7.75E-9	4.85E-9
t ₂	SiO ₂	9.6E-8	1.43E-8	7.3E-9	1.25E-9
	PBO	1.04E-7	2.24E-8	8.19E-9	2.79E-9

Partial Pressures of Contaminants (Data of Fig. 6)

increase observed at t₁, corresponds to the opening of the slit valve of the ICP etch chamber to allow wafer picking. The residual outgassing load impacts the VTM pressure even after the etched wafer is placed to the next process chamber. Initially, in the case of SiO₂ wafers (Figure 7a) only masses 40 and 20 impact the VTM pressure. In contrast, on PBO wafers (Figure 7b) the total pressure is more than one order of magnitude higher and the contribution, beside Ar, comes from all other species, except of mass 32. At the instant t₂, a wafer previously degassed in the ABD is picked from the airlock and enters the VTM. This action is accompanied by an increase of the partial pressures of mass 17 and 18, which is likely due to the outgassing of the hot wafer. Similarly, masses 28 and 32 also increase and this can be explained by the residual atmosphere of the airlock. The VTM pressure is again stable at the instant t₃; however, there is a much more significant contribution of masses 40 and 20, and in a lesser extent of mass 44, in the case of PBO wafers. This phenomenon was not observed on the HEXAGON (Figure 7b). During steady-state operation, between t₃ and t₄, one wafer remains idle on the robot arm waiting to be placed in the ICP etch chamber. Since the temperature of this wafer is still around 100°C it continues to outgas and to contaminate the VTM environment. The

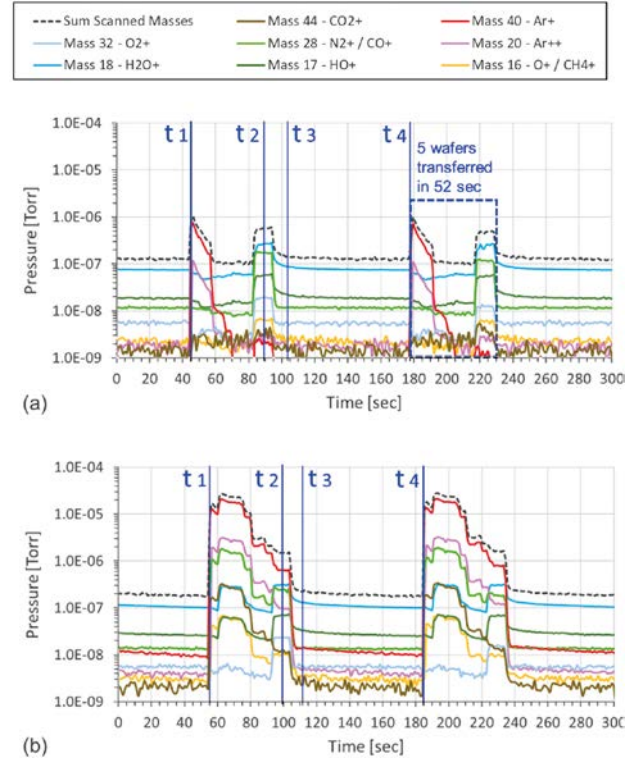


Figure 7: Selected masses measured in the CLUSTERLINE® VTM, comparison of SiO₂ wafers (a) vs. PBO wafers (b).

Time flag	Wafer type	Selected masses and partial pressures [Torr]			
		Mass 18	Mass 28	Mass 32	Mass 44
t ₁	SiO ₂	6.64E-8	1.16E-8	2.6E-9	2.2E-9
	PBO	9.93E-8	1.07E-6	4.66E-9	1.64E-7
t ₂	SiO ₂	2.71E-7	1.74E-7	1.95E-8	4.22E-9
	PBO	3.12E-7	2.48E-7	2.28E-8	1.27E-8
t ₃	SiO ₂	9.2E-8	1.18E-8	5.04E-9	1.56E-9
	PBO	1.34E-7	1.39E-8	5.81E-9	2.38E-9

Partial Pressures of Contaminants (Data of Fig. 7)

periodic time interval between t₁ and t₄ can be used to calculate the steady-state throughput with (1). Thus, a cycle time of 128.7 sec corresponds to a throughput of 28.0 wafers/hour. The throughput limitation comes from the ICP etch sequence bottleneck summed to the overhead due to the chamber-to-chamber transfer.

HEXAGON - PVD-Ti chamber RGA: SiO₂ vs. PBO Wafers

Figure 8a and 8b compare the behavior of the PVD-Ti chamber of the HEXAGON during the residence of SiO₂ and PBO wafers previously processed with ABD, cooling step and split ICP etch. The instant t₁, corresponds to the start of the down movement of the pedestal. This is accompanied by a sharp pressure increase caused by the volatile species coming from the other process chambers and by the residual atmosphere of the airlock. After the transfer, in the case of SiO₂ wafers, the total chamber pressure rapidly drops to the level indicated at t₂ and remains stable until the next indexing event takes place at t₄. Similarly, the contaminant species present remain constant during the timeframe t₂-t₄. On the other hand, one can notice a slow and steady decay of mass 40 in the same time interval.

In the case of PBO wafers, when the chamber is isolated from the VTM, such as at t2 and t3, the signal of mass 28 and 44 is almost one decade higher compared to SiO₂ (see Table V). Moreover, contrary to SiO₂, mass 40 remains the main contributor to the total pressure. The decay of mass 40 between t2 and t3, is somewhat slower compared to SiO₂. This may indicate that the film material itself and/or the surface roughness plays a role on the incorporation of Ar [15]. It is noteworthy to mention that mass 40 signal would completely disappear at t2 if no ICP etch process would have been performed, but instead only Ar gas would have been flown in the ICP etch chamber (data not shown here). This observation strongly supports the fact that Ar gets trapped in the film during the ICP etch process and is then gradually released over time.

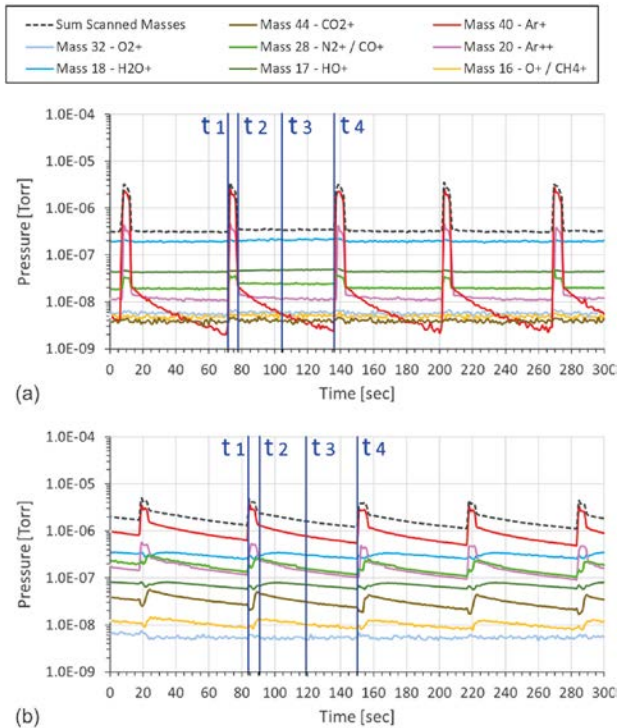


Figure 8: Selected masses measured in the PVD-Ti chamber of the HEXAGON, comparison of SiO₂ wafers (a) vs. PBO wafers (b).

Time flag	Wafer type	Selected masses and partial pressures [Torr]			
		Mass 18	Mass 28	Mass 32	Mass 44
t ₁	SiO ₂	2.11E-7	3.51E-8	6.66E-9	4.52E-9
	PBO	3.03E-7	1.86E-7	6.12E-9	2.12E-8
t ₂	SiO ₂	1.94E-7	2.59E-8	5.85E-9	4.45E-9
	PBO	2.96E-7	2.5E-7	5.9E-9	5.01E-8
t ₃	SiO ₂	2.12E-7	2.43E-8	5.71E-9	3.75E-9
	PBO	3.08E-7	1.55E-7	4.94E-9	2.99E-8

Partial Pressures of Contaminants (Data of Fig. 8)

CLUSTERLINE® – PVD-Ti chamber RGA: SiO₂ vs. PBO Wafers

Figure 9 (a) and (b) compare the RGA spectra measured in the PVD-Ti chamber of the CLUSTERLINE® during the residence of SiO₂ and PBO wafers. The typical base pressure level reached in PVD-Ti chamber reaches values in the low E-8 Torr. Due to the negligible

outgassing of the SiO₂ material, when the chamber is isolated from the VTM, (i.e., starting at t1 until t < t4), the base pressure is barely affected by the wafer presence and remains below 5.0E-8 Torr (Figure 9a). The localized pressure instability observed between t1 and t2 is due to the movement of the pedestal from the hand-off position to the process position, which brings the wafer further away from the RGA device. Between t2 and t3, mass 40 exhibits a decay in a similar fashion as described earlier in Figure 8a. During the programmed 50.0 sec of waiting, the pedestal is in the upper position and wafer rests on the chuck top surface. In this so called “process position”, the shields assembly restricts the pumping gap. As soon as the sequence time is elapsed, the pedestal moves to the hand-off position, where the pumping path opens and brings the wafer closer to the RGA. This explains the slight pressure increase starting at t3.

The residual outgassing measured on PBO coated wafers is obviously more pronounced compared to SiO₂ (Figure 9b). The total pressure remains to values above 3.0E-6 Torr during the entire residence time until t < t4. The dominating signals are masses 40 and 20, originated from Argon. These are followed, in descending

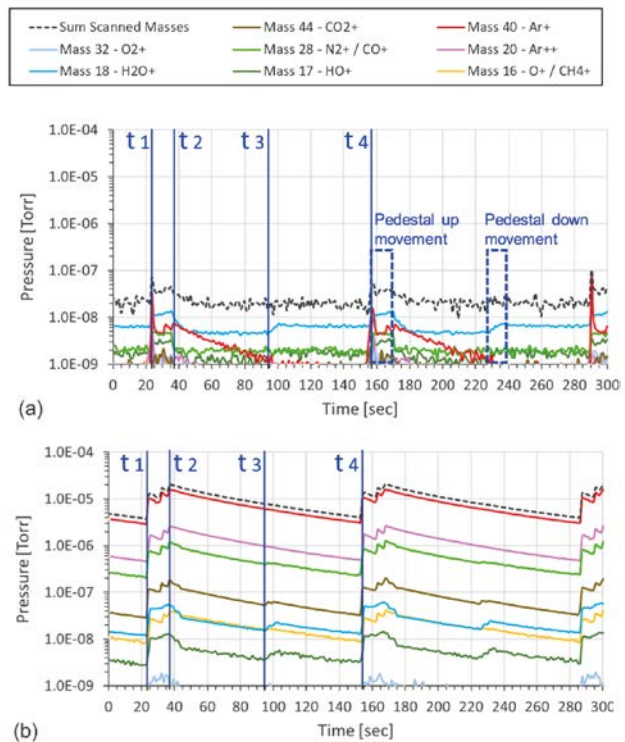


Figure 9: Selected masses measured in the CLUSTERLINE® PVD-Ti chamber, comparison of SiO₂ wafers (a) vs. PBO wafers (b).

Time flag	Wafer type	Selected masses and partial pressures [Torr]			
		Mass 18	Mass 28	Mass 32	Mass 44
t ₁	SiO ₂	1.23E-8	4.24E-9	1.16E-9	6.69E-10
	PBO	4.4E-8	7.64E-7	1.18E-9	1.17E-7
t ₂	SiO ₂	1.13E-8	2.37E-9	4.04E-10	8.46E-10
	PBO	5.25E-8	1.17E-6	1.1E-9	1.84E-7
t ₃	SiO ₂	5.71E-9	1.54E-9	2.38E-10	3.68E-10
	PBO	1.54E-8	3.98E-7	1.4E-10	5.48E-8

Partial Pressures of Contaminants (Data of Fig. 9)

order of partial pressures, by masses 28, 44, 18 and 17 (see Table VI). Similarly, to what observed on the HEXAGON, the rate of decay of masses 20 and 40 is somewhat slower on PBO than on SiO₂.

Summary

During steady-state operation, the VTM pressure of the CLUSTERLINE® is more severely impacted by the outgassing load propagating from the ICP etch chamber and from the etched wafer. This is particularly evident in the case of PBO, where the level of contaminants, especially masses 28 (CO+) and 44 (CO₂+), is almost two orders of magnitude larger compared to the HEXAGON tool. Because of the longer chamber-to-chamber transfer interval on the CLUSTERLINE®, the etched wafer may incur in a higher risk of re-contamination from its own residual outgassing. In contrast, the faster and simultaneous wafer transfer in the HEXAGON allows the VTM pressure to recover almost immediately. In this platform, the wafer type plays a less prominent role as indicated by the minor difference in the level of contaminants measured on SiO₂ and PBO.

RGA data from the PVD-Ti chambers of both platforms have shown a very different behavior on SiO₂ and PBO. In general, the contamination caused by SiO₂ wafers is almost entirely due to masses 40 (Ar+) and 20 (Ar⁺⁺). In the case of PBO wafers, the overwhelming contribution to the total pressure is as well due to masses 40 and 20, but the other contaminants are also present in a significant extent. One interesting difference is that the partial pressure of mass 40 in the CLUSTERLINE® is of order 1.0E-5 Torr, whereas in the HEXAGON it is one decade lower. Some other differences in the magnitude of the volatile contaminants can be distinguished, such as the 50% higher partial pressure of mass 28 (CO+) and mass 44 (CO+) in the CLUSTERLINE® chamber. A possible explanation is the higher wafer temperature reached during the single-step etching process performed on the ICP etch chamber of the CLUSTERLINE®, that in turn causes stronger outgassing in the PVD-Ti chamber. On the other hand, mass 18 (H₂O+) exhibits one decade lower partial pressure in the chamber

of the CLUSTERLINE®. This significant difference may be explained by the increased efficiency in the pumping of water molecules with the cryo pump, instead of the turbomolecular pump installed on the process chambers of the HEXAGON. The partial pressure of mass 32 (O₂+), is situated at approximately 1.0E-8 Torr in the HEXAGON and is not affected by the presence of the wafer in the chamber. Mass 32 is one decade lower in the CLUSTERLINE® chamber. This is in line with the better base pressure conditions.

Conclusion

A quantitative RGA benchmark between the HEXAGON and the CLUSTERLINE® would not be fair due to important HW differences, such as chamber volume, pumping efficiency (cryo vs. turbo in the PVD chambers) and the physical distance between the wafer path and the RGA device. Nevertheless, RGA measured in the vacuum transport module and the PVD-Ti chamber have provided a good picture of the cross-contamination dynamics established during steady-state operation. Experimental data has clearly shown that the main source of contamination in both systems is the residual outgassing load of the etched PBO wafer, that migrates from the etching chamber to the VTM and then accompanies the wafer to the PVD-Ti chamber. Such argument is supported by the very different behavior observed on SiO₂ and PBO films. The former does not exhibit any residual outgassing due to volatile organic contaminants.

A common phenomenon observed in both platforms is the overwhelming presence of masses 40 and 20 in the cloud of volatiles species. This may indicate that a significant amount of Argon becomes trapped in the films as a side-effect of the ICP sputter etch process. During transfer and residence in the PVD-Ti chambers, Argon is then gradually released at a different rate depending on the film material. Although the scale of the Argon presence is very significant, the investigation of the root-cause of this phenomenon is beyond the scope of this paper.

Acknowledgments

The authors would like to acknowledge Patrick Stoffel for help with RGA operation and Stephan Voser for valuable inputs in technical discussions (both at Evatec AG).

REFERENCES

- J.H. Lau, "3D IC Integration and Packaging", McGraw-Hill, New York, USA, 2016.
- B. Keser and S. Kroehnert, "Advances in Embedded and Fan-Out Wafer Level Packaging Technologies", Wiley, Hoboken, NJ, USA, 2019.
- Y. Shin and H.-O. Kim, "Analysis of Power Consumption in VLSI Global Interconnects", Proc. Int. Symposium on Circuits and Systems, 2005, pp. 4713-4716.
- P. Lianto, et al., "Under-Bump Metallization Contact Resistance (Rc) Characterization at 10-µm Polymer Passivation Opening", IEEE Trans. Components and Manufacturing Technology, Vol. 7, No 11, October 2017, pp. 1592-1597.
- Y.W. Chang, et al., "Analysis of Bump Resistance and Current Distribution of Ultra-Fine-Pitch Microbumps", Microelectronics Reliability, Vol. 53, 2013, pp. 41-46.
- C. Roberts, "Polyimide and Polybenzoxazole Technology for Wafer-Level Packaging", Chip Scale Review, July-August, 2015, pp. 26-31.
- T. Uchida and M. Furukawa, "Preparation and Properties of Rigid PBO Polymer Nanofibers Prepared via Crystallization From a Dilute Solution in Sulfuric Acid", Journal of Photopolymer Science and Technology, Vol. 27, No. 2, 2014, pp. 177-180.
- K. Furukawa and M. Ueda, "Recent Development in Photosensitive Polybenzoxazoles", Polymer J., Vol. 38, No. 5, 2006, pp. 405-418.
- P. Carazzetti, et al., "Impact of Process Control on UBM/RDL Contact Resistance for Next-Generation Fan-Out Devices", IEEE 67th Electronic Components and Technology Conference (ECTC), Orlando, FL, USA, 2017, pp. 909-916.
- C. Drechsel, et al., "Optimum Rc Control and Productivity Boost in Wafer-Level Packaging Enabled by High-Throughput UBM/RDL Technology", IEEE 73rd Electronic Components and Technology Conference (ECTC), Orlando, FL, USA, 2023, pp. 126-131.
- F. Balon, P. Carazzetti, J. Weichart, M. Elghazzali, and M. Hoffmann, "Addressing the Need of UBM/RDL Processing in FOWLP", Proc. Int. Wafer-Level Packaging Conf. (IWLPC), San Jose, CA, USA, 2016.
- B. Scholte Von Mast, W. Rietzler, R. Lodder, R. Bazlen, and D. Rohrer, U.S. Patent 10,138,553 B2, Nov. 27, 2018.
- <https://www.mks.com/f/hpq3-high-pressure-residual-gas-analyzer>
- <http://ytionline.com/technical-information/rga-spectra-data-interpretation-guide/>
- C. Biswas, A.K. Shukla, S. Banik, V.K. Ahire, and S.R. Barman, "XPS and LEED study of Argon Bombarded Al(111) Surface", Nuclear Instruments and Methods in Physics Research B 212, 2003, pp. 297-302.